


# Simulation and Observation of Magnetic Particles Captured in Fluids Using High Temperature Superconductor Bulk

Chia-Ming Yang , Wei-Hsuan Chang, Jyun-Rong Huang, and In-Gann Chen

**Abstract**—Single grained high temperature superconductor (HTS) bulks can trap a magnetic field up to approximately 17 tesla at low temperatures, which is significantly larger than that of permanent magnets (PMs) at about 0.5–1.0 tesla. This study compared the trajectory of magnetic particles using three different magnetic field sources, i.e., an HTS bulk working at 65K and 77 K and a PM, respectively. In addition, the theoretical trajectory of magnetic particles was also calculated and compared with that of the direct experimental observations, which indicated high calculation accuracy. Due to the magnetic flux density gradient differences between a PM and HTS bulk, the distributions of the magnetic particles were also different, which showed the highest density at the edge for a PM and at the center for an HTS bulk. In this report, it was shown that the HTS bulk working at 65 K resulted in a higher magnetic force that can concentrate more magnetic particles in a small area.

**Index Terms**—MDDS, magnetic force, HTS bulk, trajectory simulation.

## I. INTRODUCTION

MAGNETIC drug delivery systems (MDDS) comprise a type of therapeutic process developed in 1980 [1], that can be applied in cancer and gene therapies. Some magnetic materials such as  $\text{Fe}_3\text{O}_4$  are attached to the drugs, and the drugs are manipulated by an external magnetic field source to move to the affected area (target area). The first clinical experiment with MDDS was done in 1996, and the experimental results showed that MDDS can effectively concentrate magnetic drugs in an affected area [2], [3]. Also, it was shown that the concentration density increased with the strength of the magnetic field and the magnetic gradient. Therefore, determining how to set up a strong, effective magnetic source is a critical need in MDDS technology [4].

Generally, the maximum field strength of a permanent magnet [5] is about 1.5 tesla. In some studies, the Halbach magnet array

Manuscript received November 27, 2020; revised January 23, 2021; accepted January 27, 2021. Date of publication February 5, 2021; date of current version May 20, 2021. This work was supported in part by the National Science Council, Taiwan, under Contract MOST 108-2633-M-001-001, MOST 109-2639-M-001-001. (Corresponding author: In-Gann Chen.)

The authors are with the Department of Materials Science and Engineering, National Cheng-Kung University, Tainan 70101, Taiwan (e-mail: ingann@mail.ncku.edu.tw).

Color versions of one or more figures in this article are available at <https://doi.org/10.1109/TASC.2021.3057321>.

Digital Object Identifier 10.1109/TASC.2021.3057321

was designed using permanent magnets as the MDDS magnetic source, which showed the field strength of 4-5 tesla [6], [7].

It is well known that high-temperature bulk superconductors (HTS bulk) can trap 17.6 tesla at 29 K [8], [9] which are much larger than that of a permanent magnet array. Furthermore, an HTS bulk displays an ultra-high magnetic field gradient, which is almost 75 times higher than that obtaining using a permanent magnet at a distance of 20 mm [10]–[12]. Some studies have used the HTS bulk as the magnetic field source in MDDS applications, displayed good magnetic drug delivery results[13]–[15].

To determine the motion of a particle in MDDS, some researchers have attempted to simulate the magnetic particle trajectory in a fluid with a magnetic field [16]–[20]. Although the simulation results offered more information about the magnetic strength effects in MDDS, their accuracy has been difficult to prove. Lester *et al.* attempted to use many particles of the same size to display the trajectory and supported his calculation model, but the particles interfered with each other and affected the observation results. In this paper, we attempted to build a mathematic model to calculate the trajectory of the magnetic particles and prove it by directly observing the trajectory of the particles under different magnetic situations. Also, to determine the effects of the magnetic field and field gradient, we used a permanent magnet (PM) and homemade high temperature superconductor bulk (HTS) [21], [22] as the magnetic source and compared our results with the simulation results.

## II. EXPERIMENT

### A. Magnetic Field Distributed Calculation [23]

Based on the electromagnetic theory, the distribution of magnetization can be calculated using the surface current density ( $J_s$ ) and volume current density ( $J_v$ ). This calculation method is called the  $J_s + J_v$  model.

$B_{sz}$  (a magnetic field in z-axis originated from  $J_s$ ) above the sample can be calculated by:

$$\vec{B}_{sz} = \frac{\mu J_s b}{4\pi\rho} \varphi' \int_{-t}^0 \int_0^{2\pi} \frac{\sin \varphi' \left[ (z - z')^2 + b^2 - b\rho \sin \varphi' \right]}{\left[ p^2 + (z - z')^2 + b^2 - 2b\rho \sin \varphi' \right]^{\frac{3}{2}}} d\varphi' dz' \quad (1)$$

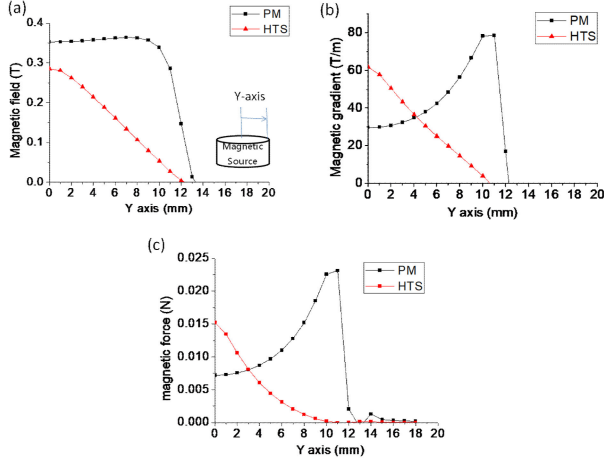


Fig. 1. (a) Magnetic field distribution and (b) magnetic gradient distribution calculated from the  $J_s + J_v$  model at a distance of 1 mm above the surface of the magnetic field source (PM and the HTS bulk). The maximum PM value was 0.35 tesla, and the maximum HTS value was 0.28 tesla. (c) The magnetic force was applied on a 1 mm iron particle using a PM and an HTS bulk as the magnetic source.

where  $\rho^2 = x^2 + y^2$ ;  $t$  is the thickness of a sample;  $b$  is the radius of a sample,  $\varphi$  is the angle for polar coordinates, and  $z$  is the distance from a sample surface.

$B_z$  due to  $J_v$  above the sample can be calculated by:

$$\vec{B}_{v_z} = \frac{\mu J_v b}{4\pi\rho} \varphi' \int_0^b \int_{-t}^0 \int_0^{2\pi} \frac{\rho' \sin \varphi' \left[ (z - z')^2 + \rho'^2 - \rho\rho' \sin \varphi' \right]}{\left[ \rho^2 + (z - z')^2 + \rho'^2 - 2\rho\rho' \sin \varphi' \right]^{\frac{3}{2}}} d\varphi' dz' d\rho' \quad (2)$$

The magnetic field ( $B_z$ ) can be described as the following:

$$\vec{B}_z = \vec{B}_{s_z} + \vec{B}_{v_z} \quad (3)$$

Fig. 1(a) shows that the magnetic field distribution of PM and HTS calculated using the  $J_s + J_v$  model. The magnetic field of a PM is relatively uniform compare to an HTS bulk.

### B. Magnetic Force Calculation

The magnetic force acting on a particle is:

$$F_m = \frac{4}{3}\pi r^3 \mu_0 (M \cdot \nabla) H \quad (4)$$

Where  $\mu_0$  is vacuum permeability;  $H$  is the magnetic field strength;  $\nabla$  is the magnetic field gradient;  $M$  is the magnetization, and  $r$  is the radius of the particle. The magnetic force acting on a 1 mm diameter iron particle can be calculated, for which the result is shown in Fig. 1(c).

### C. Trajectory of Magnetic Particle Calculation

The motion of the magnetic particle in a fluid can be described by the Basset-Boussinesq-Oseen equation if the magnetic particle falls into a low density liquid ( $\rho$ (density of the particle)  $\ll \rho_s$

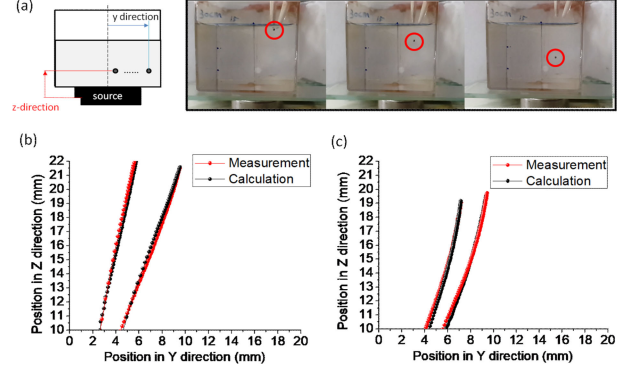


Fig. 2. (a) Schematic diagram and real images of the verify experiments. Experimental (red line) and calculated (black line) trajectories of the magnetic particles were shown using (b) PM and (c) HTS bulk as the magnetic field source.

TABLE I  
PARAMETERS USED FOR CALCULATING THE PARTICLE TRAJECTORIES

Magnetic Source				
Name	Type	Radius (m)	Thickness (m)	Magnetic field (tesla)
PM	Permanent magnet	0.12	0.10	0.35
HTS	Superconductor	0.12	0.12	0.28 (77 K) 0.87 (65 K)
Magnetic Particle				
Material	Diameter (m)	Density (kg/m <sup>3</sup> )	Saturation Magnetic Strength (A/m)	
Iron	1	7450	1.34*10 <sup>6</sup>	
Solution				
	State	Density (kg/m <sup>3</sup> )	Viscosity (kg/m*s)	
Glycerin	Static	1260	0.779	

(density of the liquid)). This equation can be simplified as follows [24]:

$$m \frac{du}{dt} - mg \left( 1 - \frac{\rho}{\rho_s} \right) - \frac{1}{8} \pi D^2 \rho C_D \mu^2 - \frac{1}{12} \pi D^3 \rho \frac{du}{dt} \quad (5)$$

Where  $D$  is the diameter of a particle;  $m$  is the mass of particle;  $\mu$  is the viscosity of the fluid;  $u$  is the particle velocity;  $t$  is time;  $g$  is the gravitational constant, and  $C_D$  is the drag coefficient.

### D. Trajectory of Magnetic Particle Calculation

To verify our calculation model, we designed an experiment to observe the trajectory of a magnetic particle. As shown in Fig. 2(a), an iron particle 1 mm in diameter was set at two positions from which to drop into the glycerin solution, which had high enough viscosity to slow down the particle. The particle was affected by the external magnetic field and gradually approached the magnetic field source (the PM or HTS bulk), resulting in a nonlinear trajectory. The entire process was recorded with an in-situ camera. The specifications of the PM and HTS bulk are shown in Table I, and the HTS bulk was worked in liquid nitrogen (77 K).

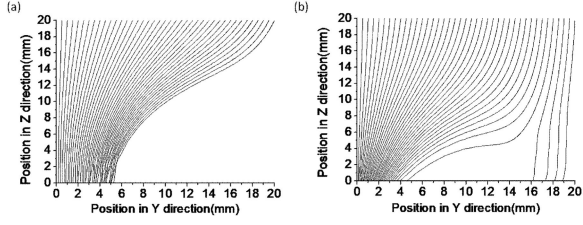


Fig. 3. Trajectory simulation of the iron particles at different positions ( $y = 1\text{--}20$  mm,  $z = 20$  mm) using the (a) PM and (b) HTS bulk as the magnetic field source.

### III. RESULTS AND DISCUSSION

#### A. Calculation Model Verification

Fig. 2(b) displays the calculation (black line) and measurement (red line) results for the trajectories of the magnetic particles using PM as the magnetic source. It shows that the red line and black line nearly overlap for different starting positions, with the largest error being  $<10\%$ . Similar results are shown in Fig. 3(c), where HTS bulk is used as the magnetic source. The findings suggest the displacements in the  $y$  direction for the HTS bulk magnetic particles were smaller than those for the PM. It should be noted that the starting positions of the particles were set at  $y = 5, 8$  mm and  $z = 20$  mm. However, due to errors caused by complications related to the experimental operations, the actual starting positions of the particles were recalibrated with the images recorded by the camera. This is why in Fig. 2(b) and (c), there are slight differences in the starting positions. Moreover, as shown in Fig. 1, it was found a large difference in the magnetic force distribution for the PM and HTS bulk. These results strongly suggest that our calculation model is reliable even under different magnetic field situations.

#### B. Trajectory Analysis for Different Magnetic Field Sources

To obtain more information, our calculation model was extended to simulate the trajectories in additional positions ( $y = 1\text{--}20$  mm,  $z = 20$  mm), as shown in Fig. 3. It was found that using PM as a magnetic field source led to the capture of all the iron particles, but HTS only captured iron particles when  $y$  was smaller than 18 mm. This could be easily explained by the fact that the magnetic force of the HTS bulk was very weak at its edge compared to that of the PM. However, if we attempted to summarize the final position ( $z = 0$ ) of the iron particles, we found that they were focused at  $y = 5$  by PM and at  $y = 0$  (center) by HTS, respectively.

The  $J_c$  of a HTS bulk at different temperature can be obtained by the exponential decay equation  $J_c = J_c(0)(1 - T/T_c)^\alpha$ , where  $J_c(0)$  is the critical current density at  $T_c$  ( $\sim 90$  K);  $T$  is working temperature;  $\alpha$  is a material constant (0.9–2) [25]. Since the trapped magnetic field is direct proportion to  $J_c$  ( $\sim J_v$  in Eq. 2), the magnetic field will increase as the working temperature is reduced from 77K to 65K. The calculated field distribution of the HTS bulk at 65K is shown in the inset of Fig. 4(a), and the maximum magnetic field strength is 0.87 T, which is about the same to previous published results [26], [27]. When an HTS bulk

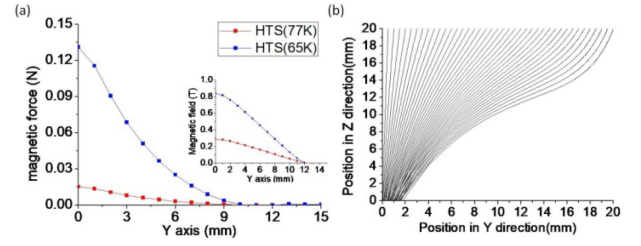


Fig. 4. (a) magnetic force and field distribution (inset) of the HTS bulk working at 77 K and 65 K; (b) Trajectory simulation of the iron particles at different positions ( $y = 1\text{--}20$  mm,  $z = 20$  mm) for the HTS bulk working at 65 K.

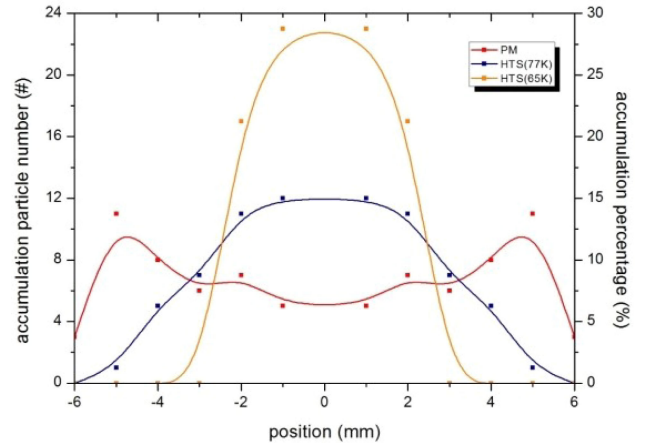


Fig. 5. The iron particle distributions (accumulation percentage) for different magnetic sources.

worked at 65 K, the magnetic force applied on an iron particle was increased six-fold, as shown in Fig. 4(a). Fig. 4(b) shows the simulation results for iron particles using the HTS bulk worked at 65 K. The findings suggest that all the iron particles were captured and that their final position ( $z = 0$ ) was denser and focused at  $y = 0$  mm.

#### C. Particle Concentration

In order to explore the advantages of the HTS bulks, we counted the number of particles in each position along the  $y$ -direction, as summarized in Fig. 5. The particle accumulation percentage was defined as the ratio of the number of magnetic particles at each position range to the total number of particles ( $n = 40$ ), and this method also presented in other research [20]. It can be clearly seen from the figure that when a permanent magnet was used as the magnetic field source, 12% of iron particles were concentrated on the edge, while in other locations, there were still the concentration of 8%. If an HTS bulk working at 77 K was used, 14% of iron particles were concentrated in the center and gradually decreased toward the edge, which still indicated a large distribution range for the magnetic particles. However, when a superconductor working at 65 K was used, because of its stronger trapped magnetic ability, the particles were obviously concentrated in the center (23%), and there were no magnetic particles out of the range of 2.5 mm away from the center.

#### IV. CONCLUSION

This study showed that the calculated trajectories concurred with the experiment results for both PM and HTS magnets, respectively. According to the simulation results, the iron particles were ultimately concentrated at  $y = 5$  mm for the PM and at the center for the HTS bulk. If we attempted to allow the HTS bulk to work at a lower temperature such as 65 K, the iron particles concentrated better at the center. For MDDS applications, determining how to more effectively concentrate drugs on the disease area is the most important problem. In this work, an HTS bulk exhibited better concentration ability at the targets (iron particles) under similar magnetic field strengths and also had a higher magnetic field when the working temperature was decreased. It is strongly suggested that the HTS bulk is more suitable for use in MDDS than the PM bulk, if the target area is very small (Diameter  $< 5$  mm). Moreover, it is no doubt that our calculation can be applied to other situations such as smaller particles or liquid flowing, but more verification experiments will be needed to prove the accuracy of the calculation in the future.

#### REFERENCES

- [1] K. J. Widder, A. E. Senyei, and D. F. Ranney, "In vitro release of biologically active adriamycin by magnetically responsive albumin microspheres," *Cancer Res*, vol. 40, pp. 3512–3517, 1980.
- [2] A. S. Lubbe *et al.*, "Clinical experiences with magnetic drug targeting: A phase I study with 4' epidoxorubicin in 14 patients with advanced solid tumors," *Cancer Res*, vol. 56, pp. 4686–4693, 1996.
- [3] A. S. Lubbe *et al.*, "Predinical experiences with magnetic drug targeting: Tolerance and efficacy," *Cancer Res*, vol. 56, pp. 4694–4701, 1996.
- [4] C. Alexiou *et al.*, "A high field gradient magnet for magnetic drug targeting," *IEEE Trans. Appl. Supercond.*, vol. 16, pp. 1527–1530, Jun. 2006.
- [5] Y. Hirota, Y. Akiyama, Y. Izumi, and S. Nishijima, "Fundamental study for development magnetic drug delivery system," *Phys. C*, vol. 469, pp. 1853–1856, 2009.
- [6] F. Bloch, O. Cugat, G. Meunier, and J. C. Toussaint, "Innovating approaches to the generation of intense magnetic fields: Design and optimization of a 4 tesla permanent magnet flux source," *IEEE Trans. Magn.*, vol. 34, no. 5, pp. 2465–2468, Sep. 1998.
- [7] M. Kumada *et al.*, "Development of 4 tesla permanent magnet," Present at *Proc. 2001 Part. Accel. Conf.* (Cat. No. 01CH37268), 2001.
- [8] M. Tomita and M. Murakami, "High-temperature superconductor bulk magnets that can trap magnetic fields of over 17 tesla at 29," *Nature*, vol. 421, pp. 517–520, 2003.
- [9] J. H. Durrell *et al.*, "A trapped field of 17.6 t in melt-processed, bulk Gd-Ba-Cu-O reinforced with shrink-fit steel," *Supercond. Sci. Technol.*, vol. 27, no. 8, 2014, Art. no. 082001.
- [10] S. Ueno and M. Iwasaka, "Properties of diamagnetic fluid in high gradient magnetic fields," *J. Appl. Phys.*, vol. 75, no. 10, pp. 7177–7179, 1994.
- [11] M. Murakami, "Progress in applications of bulk high temperature superconductors," *Supercond. Sci. Technol.*, vol. 13, p. 448, 2000.
- [12] S. Takeda, F. Mishima, S. Fujimoto, Y. Izumi, and S. Nishijima, "Development of magnetically targeted drug delivery system using superconducting magnet," *J. Magn. Magn. Mater.*, vol. 311, no. 1, pp. 367–371, 2007.
- [13] S. Fukui *et al.*, "Study on optimization design of superconducting magnet for magnetic force assisted drug delivery system," *Phys. C*, vol. 463–465, pp. 1315–1318, 2007.
- [14] S. Nishijima *et al.*, "A study of magnetic drug delivery system using bulk high temperature superconducting magnet," *IEEE Trans. Appl. Supercond.*, vol. 18, no. 2, pp. 874–877, Jun. 2008.
- [15] S. Nishijima *et al.*, "Research and development of magnetic drug delivery system using bulk high temperature superconducting magnet," *IEEE Trans. Appl. Supercond.*, vol. 19, no. 3, pp. 2257–2260, Jun. 2009.
- [16] J. Estelrich, E. Escribano, J. Queralt, and M. A. Busquets, "Iron oxide nanoparticles for magnetically-guided and magnetically-responsive drug delivery," *Int. J. Mol. Sci.*, vol. 16, no. 4, pp. 8070–8101, 2015.
- [17] S. Sharma, V. K. Katiyar, and U. Singh, "Mathematical modelling for trajectories of magnetic nanoparticles in a blood vessel under magnetic field," *J. Magn. Magn. Mater.*, vol. 379, pp. 102–107, 2015.
- [18] L. C. Barnsley, D. Carugo, M. Aron, and E. Stride, "Understanding the dynamics of superparamagnetic particles under the influence of high field gradient arrays," *Phys. Med. Biol.*, vol. 62, no. 6, 2017, Art. no. 2333.
- [19] M. Mahmoodpour, M. Goharkhah, and M. Ashjaee, "Investigation on trajectories and capture of magnetic drug carrier nanoparticles after injection into a direct vessel," *J. Magn. Magn. Mater.*, vol. 497, 2020, Art. no. 166065.
- [20] K. Nakagawa, F. Mishima, Y. Akiyama, and S. Nishijima, "Study on magnetic drug delivery system using HTS bulk magnet," *IEEE Trans. Appl. Supercond.*, vol. 22, no. 3, Jun. 2012, Art. no. 4903804.
- [21] C. M. Yang, C. H. Liu, B. X. Chen, C. W. Chang, and I. G. Chen, "Pellet-buffered film seed to grow single grain bulk YBCO," *J. Amer. Ceram. Soc.*, vol. 100, no. 11, pp. 5038–5043, 2017.
- [22] C. M. Yang, S. Y. Wang, Y. C. Huang, P. W. Chen, I. G. Chen, and M. K. Wu, "The optimal growth of single grain bulk Y–Ba–Cu–O superconductors with Nd–Ba–Cu–O thin film seed," *IEEE Trans. Appl. Supercond.*, vol. 23, no. 3, Jun. 2013, Art. no. 6800204.
- [23] I. G. Chen, J. Liu, R. Weinstein, and K. Lau, "Characterization of YBa<sub>2</sub>Cu<sub>3</sub>O<sub>7</sub>, including critical current density  $j_c$ , by trapped magnetic field," *J. Appl. Phys.*, vol. 72, no. 3, pp. 1013–1020, 1992.
- [24] M. Jalaal, D. D. Ganji, and G. Ahmadi, "Analytical investigation on acceleration motion of a vertically falling spherical particle in incompressible newtonian media," *Adv. Powder Technol.*, vol. 21, no. 3, pp. 298–304, 2010.
- [25] A. Kuznetsov, I. Sannikov, and A. Ivanov, "Temperature dependence of critical current in YBa<sub>2</sub>Cu<sub>3</sub>O<sub>7- $\delta$</sub>  films," *J. Phys. Conf. Ser.*, vol. 941, no. 1, 2017, Art. no. 012071.
- [26] M. D. Ainslie *et al.*, "Pulsed field magnetization of single-grain bulk YBCO processed from graded precursor powders," *IEEE Trans. Appl. Supercond.*, vol. 26, no. 4, Jun. 2016, Art. no. 6800104.
- [27] X. Chaud, E. Haanappel, J. G. Noudem, and D. Horvath, "Trapped field of YBCO single-domain samples using pulse magnetization from 77K to 20K," *J. Phys. Conf. Ser.*, vol. 97, 2008, Art. no. 012047.